

Application of magnetic resonance imaging *in vivo* for the assessment of the progression of systolic and diastolic dysfunction in a mouse model of dilated cardiomyopathy

Łukasz Drelicharz¹, Mirosław Woźniak¹, Tomasz Skórka², Urszula Tyrankiewicz², Sylwia Heinze-Paluchowska², Magdalena Jabłońska², Anna Gębska³, Stefan Chłopicki¹

¹ Department of Experimental Pharmacology, Chair of Pharmacology, Jagiellonian University *Collegium Medicum*, Krakow, Poland

² Department of Magnetic Resonance Imaging, Institute of Nuclear Physics, Polish Academy of Sciences, Krakow, Poland

³ Department of Pharmacological Analysis, Chair of Pharmacology, Jagiellonian University *Collegium Medicum*, Krakow, Poland

Abstract

Background: The impairment of cardiac diastolic function is essential for the development and progression of heart failure, regardless of the systolic performance of the heart. Novel methods of diagnosis of diastolic dysfunction in experimental animals are needed in order to validate the effectiveness of novel heart failure treatment.

Aim: The *in vivo* characterisation of diastolic and systolic function of the heart during heart failure progression in Tg α q*44 mice using magnetic resonance imaging (MRI) and original image analysis.

Methods: Cardiac function *in vivo* in both Tg α q*44 and FVB mice was analysed using MRI at 4.7 T. Magnetic resonance imaging was performed using an ECG triggered fast gradient echo (cine-like flow compensated FLASH) sequence. For the assessment of left ventricle (LV) dynamics at least 20 images per cardiac cycle were acquired in the midventricular short-axis projection at the level of papillary muscles. End-systolic (ESA) and end-diastolic (EDA) areas were estimated from the minimum and maximum values found in the area-time plot. Fractional area change (FAC) defined as (EDA-ESA)/EDA, ejection (ER) and filling (FR) rates defined as slope of the beginning part of the systolic and diastolic limbs were calculated. In addition, heart failure progression in Tg α q*44 mice was assessed by morphometric parameters (ventricular weight to body weight index and wet to dry lung weight index), level of BNP mRNA expression as well as survival.

Results: Systolic function assessed by FAC% and ER was stable but slightly impaired up to 10 months of age in Tg α q*44 mice as compared to the FVB mice. After 12 months of age of the Tg α q*44 mice there was a progressive deterioration of systolic function (ER at 10, 12, 14 months of age were 0.0188 ± 0.00434 , 0.0140 ± 0.00474 , 0.0115 ± 0.00469 1/ms, respectively). Diastolic function of the Tg α q*44 hearts was preserved or even slightly augmented between 4 and 10 months of age, then at the age of 12 months and later profoundly impaired (FR at 10, 12, 14 months of age were 0.0280 ± 0.01031 , 0.0196 ± 0.01050 , 0.0158 ± 0.00833 1/ms, respectively).

Conclusions: The MRI allows reliable *in vivo* assessment of the systolic and diastolic function in Tg α q*44 mice. In Tg α q*44 mice after few months of stable and compensated phase of the heart failure decompensation develops that involves impairment of both systolic and diastolic and leads to the fully symptomatic dilated cardiomyopathy. The precise molecular mechanisms of the systolic and diastolic dysfunction and their relative contribution to the heart failure progression in Tg α q*44 mice remain to be established.

Key words: diastolic dysfunction, MRI, heart failure, transgenic mice, dilated cardiomyopathy

Kardiologia Polska 2009; 67: 386-395

Introduction

Heart failure (HF) for many years was strictly linked to the systolic dysfunction of the left ventricle (LV). However, nearly 50% of patients with symptoms of chronic HF have preserved systolic LV function [1, 2]. Apart from HF with decreased ejection fraction (HFREF – heart failure with

reduced ejection fraction), a HF with normal ejection fraction (HFNEF – heart failure with normal ejection fraction) also exists. The definition of this condition is based on the coexistence of symptoms of congestive HF and normal or slightly decreased LVEF (> 50%) and the signs of diastolic dysfunction. The division into HFREF and HFNEF is far from perfect because it does not differentiate patients with HF

Address for correspondence:

Łukasz Drelicharz MD, Zakład Farmakologii Doświadczalnej, Katedra Farmakologii, Uniwersytet Jagielloński *Collegium Medicum*, ul. Grzegórzecka 16, 31-531 Kraków, tel.: +48 12 421 11 68, fax: +48 12 421 72 17, e-mail: lukaszdz@cm-uj.krakow.pl

Received: 09 October 2008. **Accepted:** 21 January 2009.

This work was supported by the Polish Ministry of Science and Higher Education (grant no. N N518 4197 33, N N401015135 and N N401 1145 33)

according to aetiology, intensity of the symptoms and prognosis. However, it has been increasingly used in the recent years. The intensity of LV systolic dysfunction does not correlate with symptoms [3, 4]. There is a suggestion that diastolic dysfunction correlates with the intensity of symptoms and frequency of hospitalisation much better than the systolic one [5, 6]. Diastolic dysfunction is a valuable parameter for risk stratification in patients with HF, independently of systolic function of the heart muscle [7].

There is a discussion whether HFNEF is a mild and early form of HFREF or if they are two separate diseases. Could be also that presentation of heart failure as more 'systolic' or 'diastolic' depends on coexisting factors (disease modifiers) such as sex, diabetes, obesity, hypertension, age and heart hypertrophy [8].

There is also no sufficient knowledge about optimal therapy of HFNEF. In contrast to the well-established methods of systolic dysfunction treatment, there are only a few studies estimating the efficacy of pharmacotherapy in reversing diastolic dysfunction of the heart muscle [9]. There are single studies showing that inhibitors of the renin-angiotensin-aldosterone system (RAAS) [10]; beta blockers [11]; nitric oxide donors (NO) [12]; statins [13]; and thiazolidinediones [14] improve the diastolic function of heart muscle. The results of new studies, investigating the efficacy of pharmacotherapy in patients with HFNEF (CHARM-Preserved [15], PEP-CHF [16]) generated new questions rather than final solutions. It seems to be necessary to work out effective methods of systolic and diastolic function evaluation in animal models of HF in vivo. This will help to understand the mechanism of diastolic dysfunction development. It will also allow the influence of HF pharmacotherapy on this function to be described in comparison to other functional, biochemical and molecular parameters.

The $Tg\alpha q^{*44}$ mice are unique animal model of HF. The overexpression of active αq subunit of the G protein in cardiomyocytes mimic persistent receptor (adrenergic $\alpha 1$, angiotensin AT_1 , endothelin ET-A) stimulation and activates the intracellular signal pathways which are known to play a key role in the pathogenesis of the heart hypertrophy and failure in humans [19].

The aim of our study was to characterise in vivo the diastolic and systolic function of the heart muscle during HF progression in $Tg\alpha q^{*44}$ using MRI technique.'

Methods

$Tg\alpha q^{*44}$ mice

In this study we used transgenic mice ($Tg\alpha q^{*44}$) 4, 8, 10, 12, 13, 14, 15 months old, which were compared to the age-matched control FVB mice. Homozygous $Tg\alpha q^{*44}$ mice and wild-type mice (FVB) were bred in the Animal Laboratory of the Polish Academy of Science Institute of Experimental and Clinical Medicine in Warsaw. Mice were housed in the pathogen-free conditions, fed a standard

laboratory diet and given water ad libitum. All of the experiments were performed according to the valid guidelines [Guide for the Care and Use of Laboratory Animals published by the US National Institutes of Health (NIH Publication No. 85-23, revised 1996)]. Approval was also obtained from the local ethics committee.

The development of HF in the $Tg\alpha q^{*44}$ mice 4, 8, 10, 12, 13, 14, and 15 months old, was studied with MRI and was completed by the measurements of BNP mRNA expression in the heart muscle and morphometric parameters of HF according to the methodology described below.

The study of mRNA expression for BNP using reverse transcriptase and polymerase chain reaction (RT-PCR)

Complete RNA was isolated from fragments of LV using TRIzol® Reagent (Gibco BRL, Life Technologies, USA) (1 mg). Then, it was reversely transcribed using reverse transcriptase (MMLV Reverse Transcriptase) and oligo (dT)12-18 (Gibco BRL, Life Technologies, USA), in the presence of dithioerythritol. The reaction of reverse transcriptase was performed in a volume of 20 µl at a temperature of 42°C for 120 min. Afterwards, the cDNA was amplified in the presence of DNA polymerase (HotStarTaq DNA Polymerase; Qiagen, USA) and a pair of specific for BNP [20] or beta-actin [21] starters. The PCR reaction was performed in a Perkin Elmer 9600 thermocycler. Products of the PCR reaction were separated electrophoretically in 2% agarose gel with addition of ethidium bromide. The further analysis was performed on the basis of images of gel made in UV light (EDAS, DC40, Kodak, USA). For densitometric evaluation of the stripes, the Scion image program (Scion Corporation, USA) was used. The results are presented in the conventional units of optical density as the proportion of optical density of stripes of mRNA for BNP to mRNA for reporter beta-actin.

Assessment of hypertrophy of heart muscle and pulmonary congestion in $Tg\alpha q^{*44}$ mouse

The mouse heart was rinsed with physiological solution and gently dried on the wiper. After cutting the atria, the ventricles were weighed. Hypertrophy of the heart was assessed according to the proportion of weight of the ventricles to weight of the mouse (VW/BW – ventricular weight to body weight index). The lungs were also removed (lower lobes of the right lung – 30-35 g). Afterwards, they were rinsed with physiological solution to remove blood clots. The next step was to dry them on the wiper. The taken fragment was weighed and left in a dryer (60°C) for 48 h and weighed again. Congestion in the pulmonary circulation was assessed on the basis of the proportion of the dry mass to the wet mass of the lung.

In vivo heart function measurement of the Tg α q*44 mouse with MR imaging

The imaging was performed with a 4.7T/310 magnet (Bruker, Germany) and MARAN DRX console (Resonance Instruments, UK). We used a dedicated gradient coil and integrated probehead with a *birdcage* type transmit-receive coil. This set was designed and built in the MRI Department of INP PAS, according to the methodology described earlier [22]. The examination was performed in the following way: during examination the mouse was anaesthetised with isoflurane (2%), oxygen and air (40 : 60%). During the examination the ECG was recorded (SA Instruments, USA) to evaluate the heart rhythm and synchronise the acquisition of the MR with the ECG. Mice in anaesthesia were positioned supine in the probehead cradle and then put into the magnet. Afterwards a series of measurements was made in order to localise the standard measuring plane (the perpendicular plane to the long axis of the LV, at the level of papillary muscles) (Figure 1)

Finally, the series of images of LV in the consecutive phases of the heart muscle cycle (Figure 2) were collected, at least 20 images per cycle, while the observation time was over 20% longer than the cycle. The slice thickness was 1.5 mm; a single image was represented as a matrix of 128 × 128 pixels, with the Field of View (FOV) equal to 30 × 30 mm². The total time of data acquisition was 2-4 min per slice depending on the quality of the image and the length of the heart cycle. All the measurements were

performed with the use of the FLASH sequence in the multislice mode for scout images or multiphase (cine) mode for scout and final dynamic measurements.

Gathered images were processed with Aphelion software (ADCIS, France-USA). Aphelion scripts had been written for semi-automatic detection, delineation and measurements of the LV endocardium area in the images. Those scripts enabled automatic processing with the possibility of manual correction in case of the algorithm failure according to the methodology described earlier [23] (Figure 3).

The slope of the time-area curve, in systole and diastole of the heart was taken as the measure of contractibility and relaxation of the LV. Those values are the ejection ratio (ER) and the filling ratio (FR) (Figure 4.). A linear regression for the points from the beginning of the systolic and diastolic phase (the ranges of changes of the section area were as follows: 75-50% – systole; 25-50% – diastole) was used to estimate the slope value. The equivalent for echocardiographic EF was the value of fractional area change – FAC%. It was measured as the difference between end-diastole area and end-systole area divided by the end-diastole area (Figure 4).

Statistical analysis

The data were statistically analysed (ANOVA, Kruskal-Wallis test). Mean values of FAC, FR and ER for Tg α q*44 mice at different ages were compared with the FVB mice. In contrast to the Tg α q*44 mice, in the FVB mice values of measured parameters were similar for different

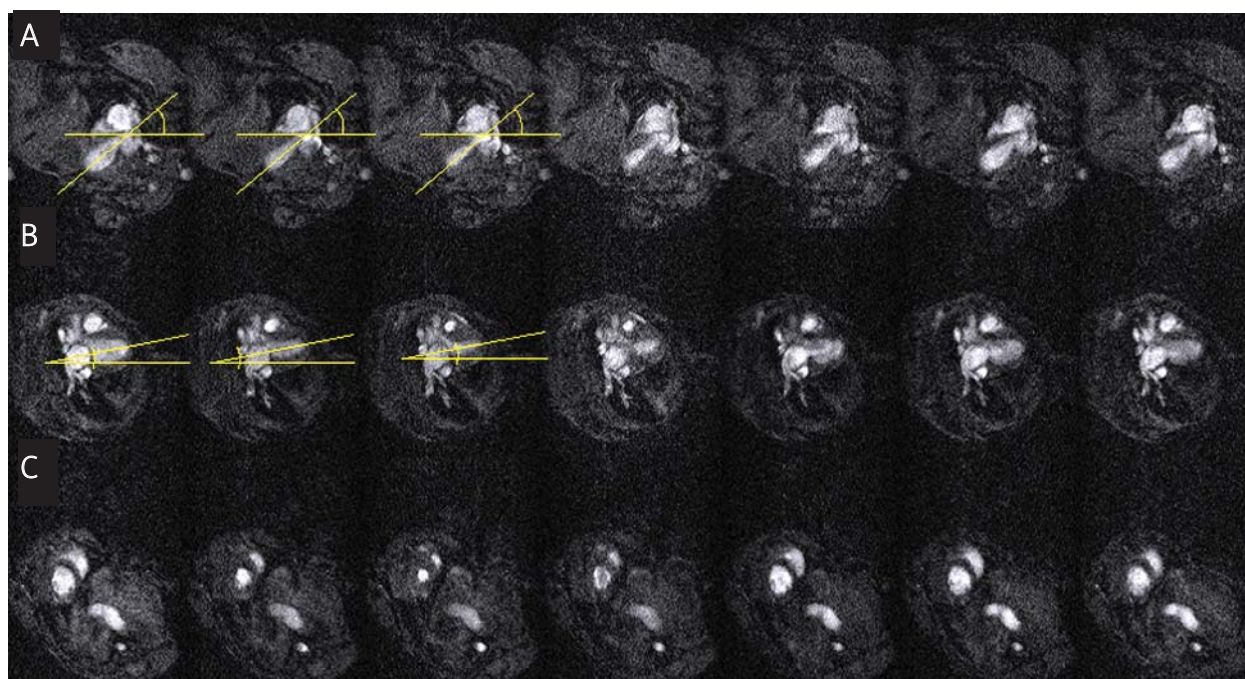


Figure 1. Positioning of the short-axis plane of mouse heart LV at the level of papillary muscles during the MRI examination. **A** – coronal view for the assignment of the first angle of the heart axis, **B** – pseudo-sagittal for the assignment of the second angle, **C** – further phases of the heart cycle in the short-axis at the level of papillary muscles

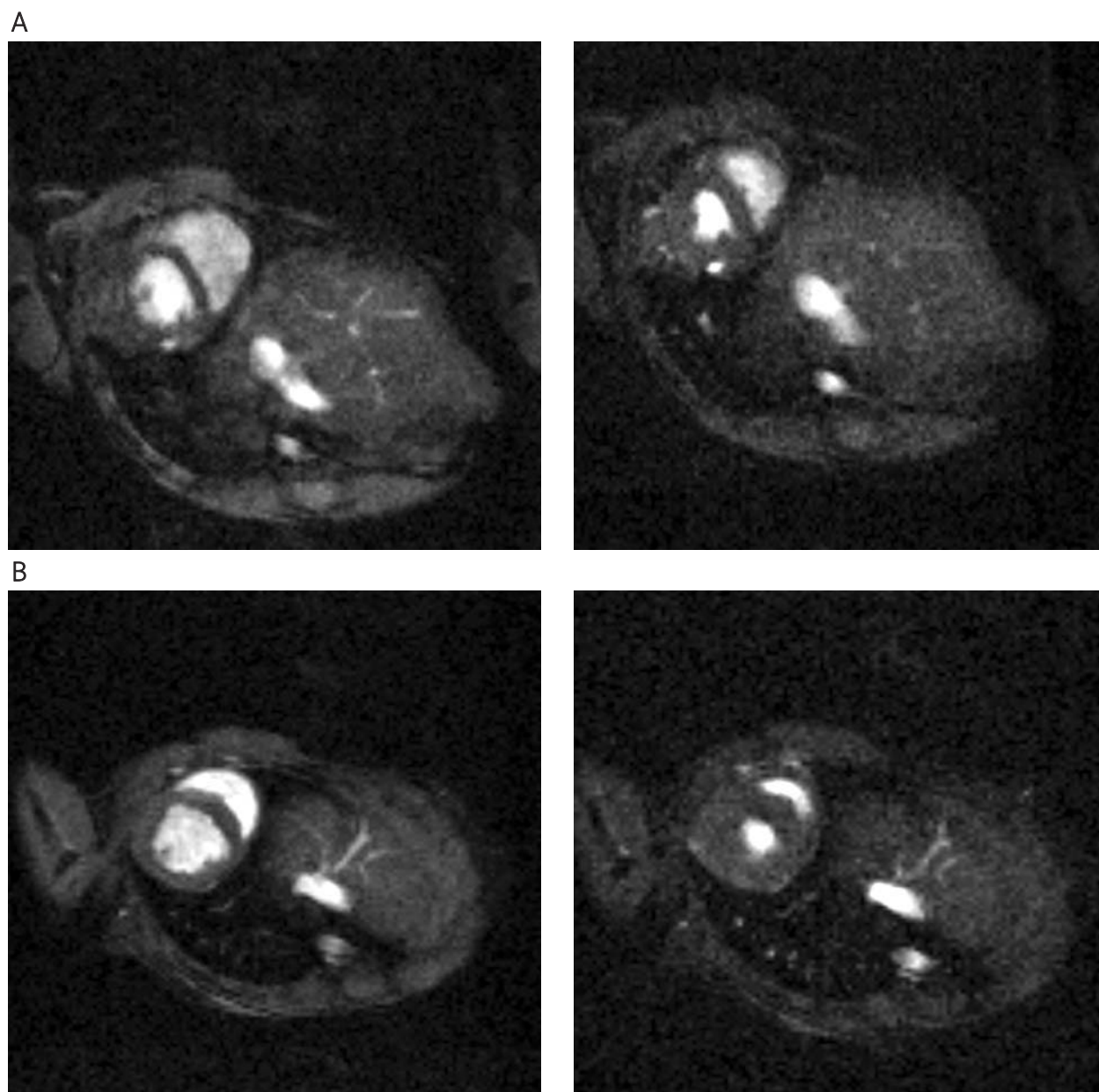


Figure 2. Examples of MR images in diastole and systole of the heart: **A** – FVB mice and **B** – Tg α q*44 mice aged 14 months. There are visible signs of dilated cardiomyopathy in the Tg α q*44 mice – marked enlargement of the RV lumen, enlarged end-systolic surface of the LV and thinning of the interventricular septum

age-groups (single-factor ANOVA, $\alpha = 0.05$). After examination of the normality of distribution (Shapiro-Wilk test) and homogeneity of the variance of analysed groups (Brown and Forsyth test), the non-parametric Kruskal-Wallis test was used for the comparisons (non-homogeneous variances between compared groups). A p value < 0.05 was considered significant.

Results

The development of HF in Tg α q*44 mice – morphometric parameters, BNP expressionAs shown in Figures 5.

A-C, the macroscopic features of HF (hypertrophy of the heart muscle, congestion in pulmonary circulation), were present only in 14- and 16-month old Tg α q*44 mice. Mortality close to 50% was observed at 16 months of life in Tg α q*44 mice (Figures 5 A-C). In the group of FVB mice there were no macroscopic signs of HF. In contrast to the delayed recognisable morphometric signs of HF in Tg α q*44 mice, the increase of expression of BNP on the level of mRNA in the heart muscle was clearly detectable in 2-month old mice. It increased during the following months with the progression of the pathology (Figure 5 D).

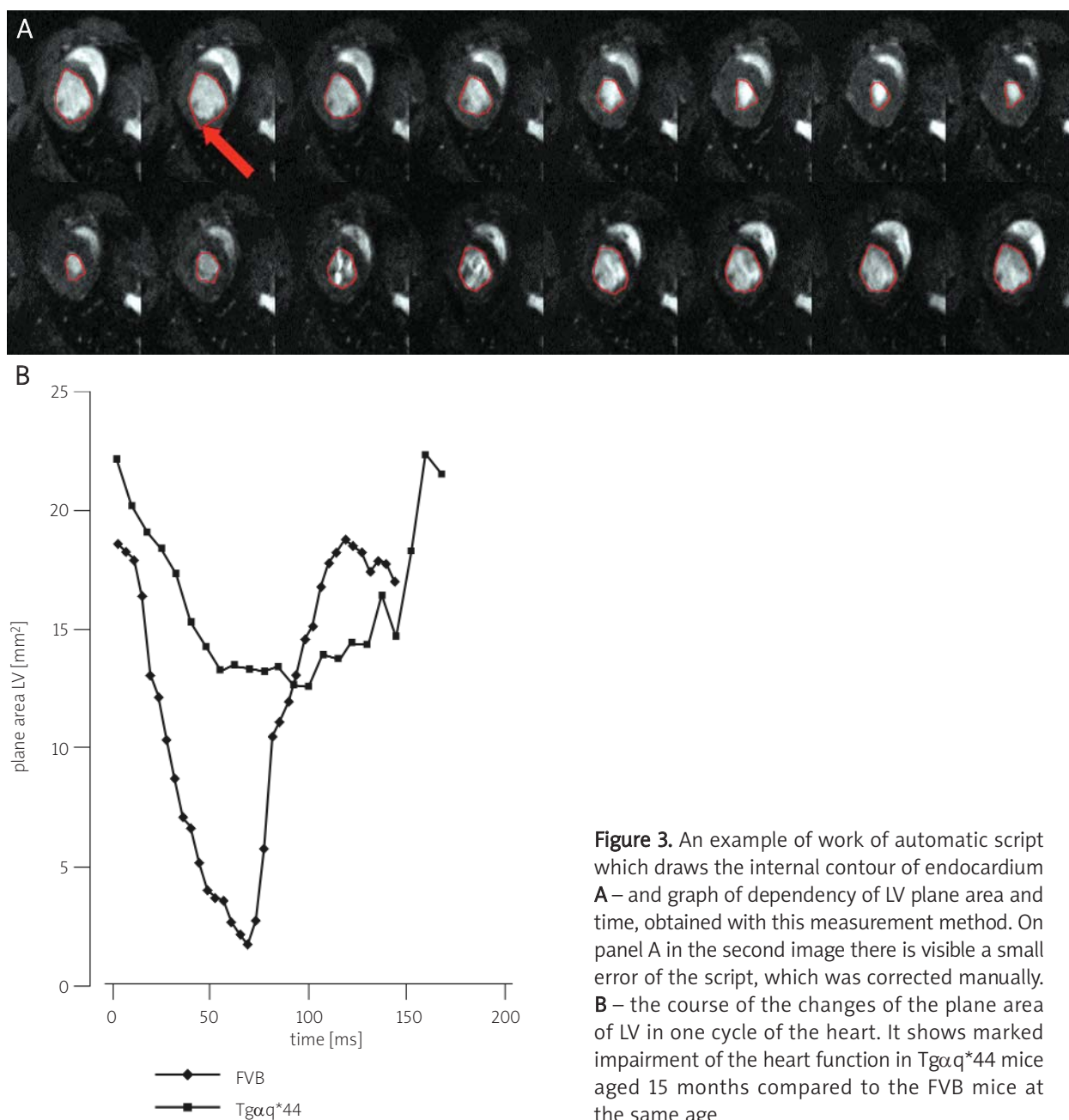


Figure 3. An example of work of automatic script which draws the internal contour of endocardium **A** – and graph of dependency of LV plane area and time, obtained with this measurement method. On panel A in the second image there is visible a small error of the script, which was corrected manually. **B** – the course of the changes of the plane area of LV in one cycle of the heart. It shows marked impairment of the heart function in Tgαq*44 mice aged 15 months compared to the FVB mice at the same age

The development of HF in Tgαq*44 – MRI study

The FAC%, ER and FR values for young and old FVB mice were not significantly different. For 4- and 16-month old mice the values were as follows: FAC 85 ± 8 vs. 83 ± 5 ; ER 0.022 ± 0.002 vs. 0.024 ± 0.003 ; FR 0.028 ± 0.008 vs. 0.023 ± 0.011 ($n = 4$). The Tgαq*44 mice aged from 4 to 10 months had the systolic activity measured as ER and FAC% at a stable level. However, in comparison to FVB mice, the FAC% values for Tgαq*44 mice were lower (75 ± 8 vs. $85 \pm 3\%$ for 4-month Tgαq*44 and FVB mice, respectively). In the older Tgαq*44 mice progressive systolic dysfunction

of LV was demonstrated (ER values in Tgαq*44 mice of the ages 10, 12, and 14 months: 0.019 ± 0.004 ; 0.014 ± 0.005 ; 0.011 ± 0.004 1/ms) (Figures 6 A, B).

The diastolic function measured as the FR was preserved (or even increased) in Tgαq*44 mice aged from 4 to 10 months. Afterwards, it decreased (FR values in Tgαq*44 mice aged 10, 12, 14 months were: 0.028 ± 0.010 ; 0.020 ± 0.010 ; 0.0160 ± 0.008 1/ms).

Discussion

The Tgαq*44 mice with overexpression of constitutively active a'q subunit in cardiomyocytes are a unique model

of slowly developing HF. The phenotype of this disease mimic the functional, biochemical and molecular signs of dilated cardiomyopathy in humans. Previously systolic dysfunction was described in $Tg\alpha q^{*44}$ mice using M-mode echocardiographic [18]. In our study we described in detail the development of changes of systolic (ER, FAC) and diastolic (FR) LV function by using original MR imaging methodology. A low degree of systolic dysfunction was observed in 4-month old $Tg\alpha q^{*44}$ mice (compared to FVB mice). It was present for the next 6 months at the same level. The mechanism responsible for primary systolic dysfunction in the $Tg\alpha q^{*44}$ mice may be directly associated with the Galphaq subunit activation and the cascade of secondary transmitters (PLC, MAP kinases, c-fos, c-myc) [17, 24-26]. However, PLC-dependent changes in the contractile units of cardiomyocytes of $Tg\alpha q^{*44}$ mice aged 12-14 months does not seem to play a key role in the development of decompensated HF [27].

The mechanisms of long-term compensated heart failure in $Tg\alpha q^{*44}$ mice are not known. One of them may be preserved or even improved LV diastolic function. This has been observed between 4 and 10 months in $Tg\alpha q^{*44}$ mice. Finally, the worsening of diastolic function in 10-12-month old mice accelerates the development of symptomatic HF. Some of these symptoms are: congestion in the pulmonary circulation, dilation of the heart muscle and a notable increase of BNP expression.

Many factors which may contribute to the diastolic dysfunction development such as fibrosis [28], changes of the isoforms of the cytoskeletons and contractile proteins [29], disturbances of intracellular calcium cycling [30, 31], coronary endothelial dysfunction [32], mitochondrial and ATP cycle dysfunction [33-35] were previously described. However, changes in expression and function of contractile proteins [decrease of troponine I phosphorylation related to decrease of activity of phosphokinase A (PKA)] [27], changes in intracellular calcium cycle [Mackiewicz et al. in the pipeline] and coronary endothelial dysfunction [36] appeared late only in 14 month old $Tg\alpha q^{*44}$ mice. The above-mentioned functional changes cannot be a causative factor of the diastolic dysfunction. They are rather secondary effects of the impaired haemodynamics of the $Tg\alpha q^{*44}$ mice heart.

Only fibrosis and mitochondrial dysfunction develop prior to the decrease of the diastolic function, and may be causative factors. The fibrosis starts at the age of 4 months and gradually intensifies (unpublished results). The mitochondrial function remains normal until 8 months and starts to be impaired in 10-month old $Tg\alpha q^{*44}$ mice [37]. This age coincides with the dysfunction of relaxation described in our study. It seems possible that impairment of energy management may play a key role in the development of diastolic dysfunction and the breakdown of the compensation mechanisms and gradual progression of HF to the decompensation phase [36, 38]. The causative

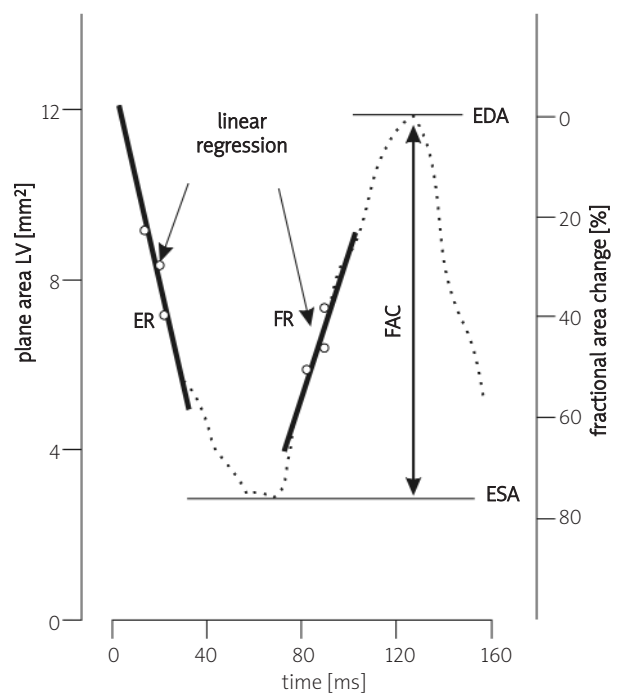


Figure 4. Methodology of measuring the functional parameters from the graph of dependency between the plane area of LV and time. For the evaluation of LV function the following parameters were used:

1. FAC% (fractional area change) = $\frac{[(EDA - ESA) / EDA] \times 100\%}{}$. EDA – end-diastole area of LV; ESA – end-systole plane area of LV;
2. ER – ejection rate (indicator of systolic dynamics) – measured as the angle of the inclination of the straight line (linear regression) drawn on the descending arm of the curve (systolic phase);
3. FR – filling rate (indicator of diastolic dynamics) – measured as the angle of the inclination of the straight line (linear regression) drawn on the ascending arm of the curve (diastolic phase)

relationship between the dysfunction of mitochondria in cardiomyocytes and diastolic dysfunction with progression of HF in $Tg\alpha q^{*44}$ mice needs further studies, especially precise analysis of the development of energetic disturbances of heart muscle.

To summarise, in this study we described for the first time the development of systolic and diastolic dysfunction in $Tg\alpha q^{*44}$ mice using in vivo MR imaging technique and worked up measurement methodology. The presented results showed that both systolic and diastolic dysfunction appeared during HF progression in $Tg\alpha q^{*44}$ mice. It seems that the diastolic one may play the key role in the development of fully symptomatic HF in this model. That is why it is a very

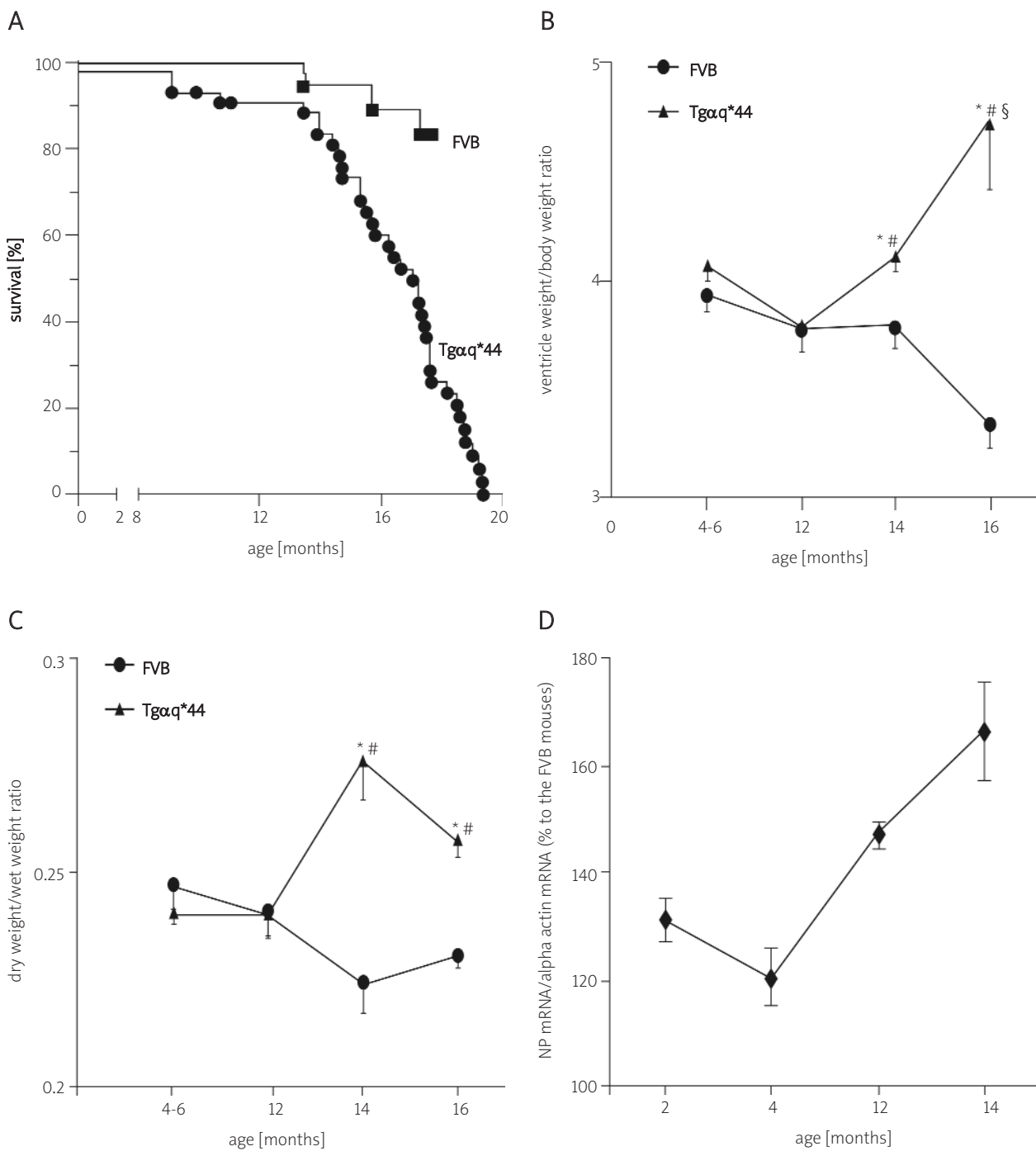
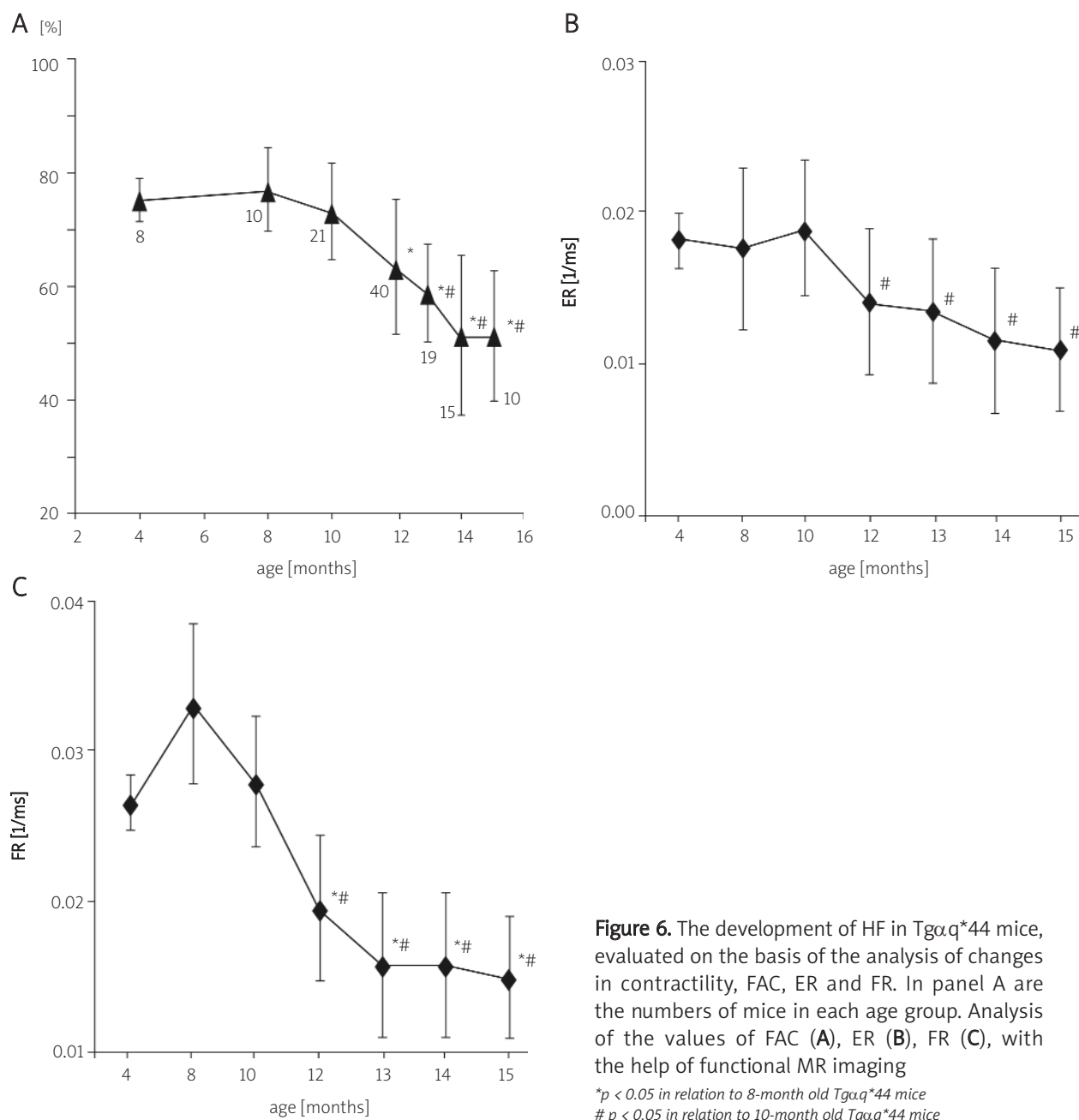


Figure 5. Progression of heart pathology in Tgαq*44 mice. **A** – survival curve of Tgαq*44 mice in comparison to FVB mice. **B** – hypertrophy of the heart presented as the ratio: ventricle weight/body weight (VW/BW), n = 5-22. **C** – congestion in pulmonary circulation presented as the ratio: dry weight/wet weight of the lung, n = 3-6. **D** – expression of BNP mRNA in the heart of Tgαq*44 mice. The results are presented as the % of expression of BNP mRNA in Tgαq*44 mice to the FVB mice at the same age (n = 5)

$p < 0.05$ vs. FVB

* $p < 0.05$ vs. Tgαq*44 (12 months old)

§ $p < 0.05$ vs. Tgαq*44 (14 months old)



interesting target for experimental pharmacotherapy of diastolic HF. However, the molecular mechanisms of systolic and diastolic dysfunction of LV and co-existing impairment of the right ventricular function need further studies.

References

- Paulus WJ, Tschope C, Sanderson JE, et al. How to diagnose diastolic heart failure: a consensus statement on the diagnosis of heart failure with normal left ventricular ejection fraction by the Heart Failure and Echocardiography Associations of the European Society of Cardiology. *Eur Heart J* 2007; 28: 2539-50.
- Rozentryt P, Nowak J, Sikora J, et al. Cardiomyopathy, asymptomatic dysfunction, acute and chronic heart failure – what does it mean in light of recent guidelines and statements? *Kardiol Pol* 2008; 66: 200-6.
- Gulec S, Ertas F, Tutar E, et al. Exercise performance in patients with dilated cardiomyopathy: relationship to resting left ventricular function. *Int J Cardiol* 1998; 65: 247-53.
- Kowalska A, Łoboz-Grudzień K, Hirmler T, et al. Left ventricular diastolic function evaluated by Doppler echocardiography in coronary artery disease in relation to systolic function. *Pol Arch Med Wewn* 1999; 102: 855-63.
- Skaluba SJ, Litwin SE. Mechanisms of exercise intolerance: insights from tissue Doppler imaging. *Circulation* 2004; 109: 972-7.

6. Hadano Y, Murata K, Yamamoto T, et al. Usefulness of mitral annular velocity in predicting exercise tolerance in patients with impaired left ventricular systolic function. *Am J Cardiol* 2006; 97: 1025-8.
7. Bhatia RS, Tu JV, Lee DS, et al. Outcome of heart failure with preserved ejection fraction in a population-based study. *N Engl J Med* 2006; 355: 260-9.
8. Fischer M, Baessler A, Hense HW, et al. Prevalence of left ventricular diastolic dysfunction in the community. Results from a Doppler echocardiographic-based survey of a population sample. *Eur Heart J* 2003; 24: 320-8.
9. Skóra E, Bilińska ZT. New therapeutic goals – new drugs in heart failure treatment. *Kardiologia Polska* 2007; 65: 1368-75.
10. Fujii M, Wada A, Tsutamoto T, et al. Bradykinin improves left ventricular diastolic function under long-term angiotensin-converting enzyme inhibition in heart failure. *Hypertension* 2002; 39: 952-7.
11. Palazzuoli A, Quatrini I, Vecchiato L, et al. Left ventricular diastolic function improvement by carvedilol therapy in advanced heart failure. *J Cardiovasc Pharmacol* 2005; 45: 563-8.
12. Matter C M, Mandinov L, Kaufmann PA, et al. Effect of NO donors on LV diastolic function in patients with severe pressure-overload hypertrophy. *Circulation* 1999; 99: 2396-401.
13. Chen Y, Ohmori K, Mizukawa M, et al. Differential impact of atorvastatin vs. pravastatin on progressive insulin resistance and left ventricular diastolic dysfunction in a rat model of type II diabetes. *Circ J* 2007; 71: 144-52.
14. Patel C, Wyne KL, McGuire DK. Thiazolidinediones, peripheral oedema and congestive heart failure: what is the evidence? *Diab Vasc Dis Res* 2005; 2: 61-6.
15. Yusuf S, Pfeffer MA, Swedberg K, et al. Effects of candesartan in patients with chronic heart failure and preserved left-ventricular ejection fraction: the CHARM-Preserved Trial. *Lancet* 2003; 362: 777-81.
16. Cleland JG, Tendera M, Adamus J, et al. Perindopril for elderly people with chronic heart failure: the PEP-CHF study. The PEP investigators. *Eur J Heart Fail* 1999; 1: 211-7.
17. Mende U, Kagen A, Meister M, et al. Signal transduction in atria and ventricles of mice with transient cardiac expression of activated G protein alpha (q). *Circ Res* 1999; 85: 1085-91.
18. Mende U, Semsarian C, Martins DC, et al. Dilated cardiomyopathy in two transgenic mouse lines expressing activated G protein alpha (q): lack of correlation between phospholipase C activation and the phenotype. *J Mol Cell Cardiol* 2001; 33: 1477-91.
19. Mann DL. Pathophysiology of Heart Failure. In: Libby P, Bonow RO, Mann DL, Zipes DP. Braunwald's heart disease a textbook of cardiovascular medicine. *Saunders Elsevier* 2008, 541
20. LaPointe MC, Mendez M, Leung A, et al. Inhibition of cyclooxygenase-2 improves cardiac function after myocardial infarction in the mouse. *Am J Physiol Heart Circ Physiol* 2004; 286: H1416-24.
21. Gebeska A, Olszanecki R, Korbut R. Endotoxaemia in rats: role of leukocyte sequestration in rapid pulmonary nitric oxide synthase-2 expression. *J Physiol Pharmacol* 2005; 56: 299-311.
22. Heinze-Paluchowska S, Skórka T, Drelicharz Ł, et al. MR imaging of mouse heart in vivo using a specialized probehead and gradient system. *Pol J Chem* 2006; 80: 1133-9.
23. Kosecka S, Wojnar L, Petryniak R, et al. Application of image analysis for quantification of cardiac function in vivo by MRI in the mouse model of heart failure. *Inżynieria Materiałowa* 2008; 4: 459-62.
24. Bowling N, Walsh RA, Song G, et al. Increased protein kinase C activity and expression of Ca²⁺-sensitive isoforms in the failing human heart. *Circulation* 1999; 99: 384-91.
25. D'Angelo DD, Sakata Y, Lorenz JN, et al. Transgenic Galphaq overexpression induces cardiac contractile failure in mice. *Proc Natl Acad Sci U S A* 1997; 94: 8121-6.
26. Takeishi Y, Chu G, Kirkpatrick DM, et al. In vivo phosphorylation of cardiac troponin I by protein kinase Cbeta2 decreases cardiomyocyte calcium responsiveness and contractility in transgenic mouse hearts. *J Clin Invest* 1998; 102: 72-8.
27. Edes IF, Toth A, Csanyi G, et al. Late-stage alterations in myofibrillar contractile function in a transgenic mouse model of dilated cardiomyopathy (Tgalphaq*44). *J Mol Cell Cardiol* 2008; 45: 363-72.
28. Burlew BS, Weber KT. Cardiac fibrosis as a cause of diastolic dysfunction. *Herz* 2002; 27: 92-8.
29. van Heerebeek L, Borbely A, Niessen HW, et al. Myocardial structure and function differ in systolic and diastolic heart failure. *Circulation* 2006; 113: 1966-73.
30. Schmidt U, Hajjar RJ, Helm PA, et al. Contribution of abnormal sarcoplasmic reticulum ATPase activity to systolic and diastolic dysfunction in human heart failure. *J Mol Cell Cardiol* 1998; 30: 1929-37.
31. Cory CR, Grange RW, Houston ME. Role of sarcoplasmic reticulum in loss of load-sensitive relaxation in pressure overload cardiac hypertrophy. *Am J Physiol* 1994; 266: H68-78.
32. Elesber AA, Redfield MM, Rihal CS, et al. Coronary endothelial dysfunction and hyperlipidemia are independently associated with diastolic dysfunction in humans. *Am Heart J* 2007; 153: 1081-7.
33. Fosslien E. Review: mitochondrial medicine – cardiomyopathy caused by defective oxidative phosphorylation. *Ann Clin Lab Sci* 2003; 33: 371-95.
34. Diamant M, Lamb HJ, Groeneveld Y, et al. Diastolic dysfunction is associated with altered myocardial metabolism in asymptomatic normotensive patients with well-controlled type 2 diabetes mellitus. *J Am Coll Cardiol* 2003; 42: 328-35.
35. Flarsheim CE, Grupp IL, Matlib MA. Mitochondrial dysfunction accompanies diastolic dysfunction in diabetic rat heart. *Am J Physiol* 1996; 271: H192-202.
36. Drelicharz Ł, Kozłowski V, Skórka T, et al. NO and PGI (2) in coronary endothelial dysfunction in transgenic mice with dilated cardiomyopathy. *Basic Res Cardiol* 2008; 103: 417-30.
37. Elas M, Bielańska J, Pustelny K, et al. Detection of mitochondrial dysfunction by EPR technique in mouse model of dilated cardiomyopathy. *Free Radic Biol Med* 2008; 45: 321-8.
38. Vogt AM, Kubler W. Heart failure: is there an energy deficit contributing to contractile dysfunction? *Basic Res Cardiol* 1998; 93: 1-10.

Zastosowanie rezonansu magnetycznego do oceny rozwoju zaburzeń czynności skurczowej i rozkurczowej mięśnia sercowego w mysim modelu kardiomiopatii rozstrzeniowej

Łukasz Drelicharz¹, Mirosław Woźniak¹, Tomasz Skórka², Urszula Tyrankiewicz², Sylwia Heinze-Paluchowska², Magdalena Jabłońska², Anna Gębska³, Stefan Chłopicki¹

¹Zakład Farmakologii Doświadczalnej, Katedra Farmakologii, Uniwersytet Jagielloński *Collegium Medicum*, Kraków

²Zakład Tomografii Magnetyczno-Rezonansowej, Instytut Fizyki Jądrowej Polskiej Akademii Nauk, Kraków

³Zakład Analizy Farmakologicznej, Katedra Farmakologii, Uniwersytet Jagielloński *Collegium Medicum*, Kraków

Streszczenie

Wstęp: Upośledzenie czynności rozkurczowej mięśnia sercowego, bez względu na wielkość frakcji wyrzutowej, odgrywa główną rolę w patogenezie niewydolności serca (ang. *heart failure*, HF). Poszukiwane są nowe sposoby obrazowania dysfunkcji rozkurczowej w modelach zwierzęcych HF oraz nowe metody jej farmakoterapii.

Cel: Scharakteryzowanie czynności skurczowej i rozkurczowej mięśnia lewej komory (LV) w toku rozwoju HF u myszy Tg α q*44 z zastosowaniem opracowanej metodyki obrazowania serca myszy *in vivo* z wykorzystaniem rezonansu magnetycznego (MRI).

Metody: Badania czynności LV u myszy Tg α q*44 na różnym etapie zaawansowania HF wykonywano metodą MRI *in vivo*. Pomiar przeprowadzono w znieczuleniu ogólnym (izofluran). Stosowano sekwencję typu FLASH, otrzymując minimum 20 obrazów pojedynczej warstwy (poziom mięśni brodawkowatych) na jeden cykl pracy serca. Czynność skurczową oceniano na podstawie wartości odcinkowej zmiany powierzchni (ang. *fractional area change*, FAC) oraz odcinkowej zmiany kurczliwości w fazie skurczu (ang. *ejection ratio* ER), a czynność rozkurczową na podstawie analogicznej wartości FR (ang. *filling ratio*). Równocześnie oceniano progresję HF u myszy Tgalafaq*44 na podstawie ich przeżycia, parametrów morfometrycznych serca (VW/BV), obrzęku płuc (mokra/sucha masa płuc) oraz ekspresji mózgowego peptydu natriuretycznego (BNP) w mięśniu sercowym.

Wyniki: Czynność skurczowa mięśnia LV oceniana na podstawie FAC% i ER utrzymywała się na podobnym poziomie w okresie od 4. do 10. miesiąca życia myszy Tg α q*44. Od 12. miesiąca czynność skurczowa stopniowo się pogarszała (wartości ER w 10., 12., 14. miesiącu życia wynosiły odpowiednio: 0,019 \pm 0,004, 0,014 \pm 0,005, 0,012 \pm 0,005 1/ms). Również czynność rozkurczowa LV (FR) była zachowana lub nawet zwiększona w okresie od 4. do 10. miesiąca życia myszy Tg α q*44, a jej upośledzenie widoczne było od 12. miesiąca życia (wartości FR w 10., 12., 14. miesiącu życia wynosiły odpowiednio: 0,028 \pm 0,010, 0,020 \pm 0,010, 0,016 \pm 0,008 1/ms).

Wnioski: Metoda MRI pozwala niezależnie ocenić zaburzenia czynności skurczowej i rozkurczowej mięśnia sercowego myszy *in vivo*. U myszy Tg α q*44 po wielomiesięcznym okresie skompensowanej HF rozwija się faza dekompensacji, która obejmuje zarówno upośledzenie czynności skurczowej, jak i rozkurczowej mięśnia sercowego i prowadzi do objawów kardiomiopatii rozstrzeniowej. Mechanizmy molekularne zmian czynności skurczowej i rozkurczowej u myszy Tg α q*44 i rola każdego z tych procesów w rozwoju zdekompensowanej HF wymagają wyjaśnienia.

Słowa kluczowe: rozkurczowa niewydolność serca, MRI, niewydolność serca, myszy transgeniczne, kardiomiopatia rozstrzeniowa

Kardiologia Polska 2009; 67: 386-395

Adres do korespondencji:

dr n. med. Łukasz Drelicharz, Zakład Farmakologii Doświadczalnej, Katedra Farmakologii, Uniwersytet Jagielloński *Collegium Medicum*, ul. Grzegorzewska 16, 31-531 Kraków, tel.: +48 12 421 11 68, faks: +48 12 421 72 17, e-mail: lukaszdz@cm-uj.krakow.pl

Praca wpłynęła: 09.10.2008. Zaakceptowana do druku: 21.01.2009.